Computing diffraction anomalies as nonlinear eigenvalue problems

Zitao Mai and Ya Yan Lu*
Department of Mathematics, City University of Hong Kong, Kowloon, Hong Kong, China

(Received 16 June 2022; accepted 31 August 2022; published 12 September 2022)

When a plane electromagnetic wave impinges on a diffraction grating or other periodic structures, reflected and transmitted waves propagate away from the structure in different radiation channels. A diffraction anomaly occurs when the outgoing waves in one or more radiation channels vanish. Zero reflection, zero transmission, and perfect absorption are important examples of diffraction anomalies, and they are useful for manipulating electromagnetic waves and light. Since diffraction anomalies appear only at specific frequencies and/or wave vectors, and may require the tuning of structural or material parameters, they are relatively difficult to find by standard numerical methods. Iterative methods may be used, but good initial guesses are required. To determine all diffraction anomalies in a given frequency interval, it is necessary to repeatedly solve the diffraction problem for many frequencies. In this paper, an efficient numerical method is developed for computing diffraction anomalies. The method relies on nonlinear eigenvalue formulations for scattering anomalies and solves the nonlinear eigenvalue problems by a contour-integral method. Numerical examples involving periodic arrays of cylinders are presented to illustrate the new method.

DOI: 10.1103/PhysRevE.106.035304

I. INTRODUCTION

For diffraction gratings and other periodic structures, transmission and reflection spectra often have interesting and useful features, such as sharp peaks and dips, flat bands, and rapid variation from a peak to a dip [1–3]. For structures without material loss, especially when the structures have relevant symmetry, it is possible to have zero reflection (total transmission) or zero transmission (total reflection) for some special frequency and wave vector [4]. It is also widely observed that a peak and a dip may appear close to each other forming an asymmetric line shape, a phenomenon called Fano resonance [2–5]. For lossy periodic structures, a particular incident wave may induce no reflected and transmitted waves, giving rise to perfect absorption [6]. When there are more than one propagating diffraction orders, it is sometimes possible to force reflected (or transmitted) wave to a particular diffraction order, leading to the so-called blazing diffraction phenomenon [7]. These and other special diffraction conditions are often referred to as diffraction anomalies, and they have been extensively investigated both theoretically and experimentally [8].

To investigate their properties and realize their applications, efficient numerical methods are needed to calculate diffraction anomalies. The diffraction of a time-harmonic incident wave by a given periodic structure is a boundary value problem (BVP). Many numerical methods have been developed to solve this BVP [9–14]. Its general solution can be represented by a scattering matrix. As we shall show in Sec. II, every diffraction anomaly is equivalent to a condition on one or more entries of the scattering matrix. Therefore, the diffraction anomalies may be found by searching the frequency (or wave vector, or other parameters) iteratively. In each iteration, the BVP is solved to find some entries of the scattering matrix. Such an iterative scheme is widely used, but it may fail if good initial guesses are not available. In addition, if all diffraction anomalies (of certain type) in a given frequency interval are required, then it is necessary to densely scan the frequency interval. The problem becomes more complicated if the diffraction anomaly only exists when some structural parameters are properly tuned. Clearly, the existing method for computing diffraction anomalies is not very reliable and computationally expensive.

In this paper, we consider a few diffraction anomalies, including zero reflection, zero transmission, perfect absorption, and blazing diffraction, and reformulate all of them as a nonlinear eigenvalue problem (NEP)

$$A(\omega)\mathbf{u} = \mathbf{0}, \tag{1}$$

where A is an operator that can be approximated by a square matrix and ω is the unknown frequency (the eigenvalue) that appears in A nonlinearly. For Eq. (1) to have a nonzero solution $\mathbf{u}$, the operator $A(\omega)$ must be singular. This implies that ω can be solved from conditions such as $\det A(\omega) = 0$ or $\sigma_1(A(\omega)) = 0$, where σ_1 is the smallest singular value of A. However, such a method also requires good initial guesses and has similar disadvantages as the iterative method based on the scattering matrix. Our approach is to solve the NEP by the contour-integral method developed by Asakura *et al.* [15] and Beyn [16]. The method allows us to find all eigenvalues of Eq. (1) inside a closed contour in the complex plane of ω. Since no initial guesses are needed, the method is robust and reliable.

The rest of this paper is organized as follows. In Sec. II, we introduce the diffraction problem and scattering matrix and identify the diffraction anomalies as special conditions on

*mayylu@cityu.edu.hk

one or more entries of the scattering matrix. In Sec. III, the diffraction anomalies are reformulated as NEPs. Numerical examples for periodic arrays of circular cylinders are presented in Sec. IV. The paper is concluded with a few remarks in Sec. V.

II. DIFFRACTION ANOMALIES

In a two-dimensional (2D) structure that is translationally invariant in spatial variable x, a polarized electromagnetic wave is also invariant in x and has only one nonzero component, namely the x component, in its electric or magnetic field. We consider an E-polarized time-harmonic electromagnetic wave in a 2D structure with a single periodic direction. The structure is periodic in y, finite in z, and surrounded by air. The dielectric function ϵ of the structure satisfies

$$\epsilon(y+L,z)=\epsilon(y,z), \quad \forall (y,z)\in\mathbb{R}^2, \tag{2}$$

$$\epsilon(y,z)=1, \quad |z|>d, \tag{3}$$

where L is the period in the y direction and $2d$ is the thickness of the structure. The x component of the electric field, denoted as u, satisfies

$$\partial_y^2 u+\partial_z^2 u+k_0^2\epsilon(y,z)\,u=0, \tag{4}$$

where $k_0=\omega/c$ is the free space wave number, ω is the angular frequency, c is the speed of light in vacuum, and the time dependence is $e^{-i\omega t}$.

A diffraction problem can have one or more plane incident waves illuminating on the periodic structure. We assume the incident waves are associated with a fixed frequency ω and a fundamental wave number $\beta\in(-\pi/L,\pi/L]$ for the y direction. Due to the periodicity, for any integer m, $\beta_m=\beta+2\pi m/L$ is a compatible wave number, and the associated plane wave is the mth diffraction order. For each integer m, $\gamma_m=\sqrt{k_0^2-\beta_m^2}$ is either real (non-negative) or pure imaginary. We assume there is a set of integers $\mathbb{M}$ containing 0, such that if $m\in\mathbb{M}$, then $\gamma_m>0$, and if $m\notin\mathbb{M}$, then $\gamma_m=i\mu_m$ for $\mu_m>0$. For $m\in\mathbb{M}$ and $m\notin\mathbb{M}$, the plane waves with wave vectors $(\beta_m,\pm\gamma_m)$ are propagating and evanescent diffraction orders, respectively. The diffraction problem can be studied with incident waves containing all propagating diffraction orders and given above and below the periodic layer (i.e., for $z>d$ and $z<-d$, respectively). For $|z|\geqslant d$, we can write down the solution of a diffraction problem as

$$u(y,z)=u^{\pm}_{\rm inc}(y,z)+u^{\pm}_{\rm sca}(y,z), \quad \pm z\geqslant d, \tag{5}$$

where the superscripts "+" and "−" signify waves above and below the periodic layer, respectively, and the subscripts indicate incident and scattered waves, respectively. Moreover, the incident and scattered waves can be expanded in plane waves as

$$u^{\pm}_{\rm inc}(y,z)=\sum_{m\in\mathbb{M}} a_m^{\pm}e^{i(\beta_m y\mp\gamma_m z)}, \tag{6}$$

$$u^{\pm}_{\rm sca}(y,z)=\sum_{m\in\mathbb{Z}} b_m^{\pm}e^{i(\beta_m y\pm\gamma_m z)}, \tag{7}$$

where $\mathbb{Z}$ is the set of all integers, $a_m^{\pm}$ for $m\in\mathbb{M}$, are given coefficients of the incident plane waves, and $b_m^{\pm}$ for all m are the coefficients of the outgoing propagating or evanescent plane waves.

The scattering matrix S maps the coefficients of the incident waves to the coefficients of the outgoing propagating waves, namely

$$\begin{bmatrix}\mathbf{b}^+\\ \mathbf{b}^-\end{bmatrix}=S\begin{bmatrix}\mathbf{a}^+\\ \mathbf{a}^-\end{bmatrix}, \tag{8}$$

where $\mathbf{a}^+$ is a column vector of a_m^+ for all $m\in\mathbb{M}$, $\mathbf{b}^+$ is a column vector of b_m^+ for all $m\in\mathbb{M}$, and so on. Let M be the number of integers in $\mathbb{M}$; then S is a $(2M)\times(2M)$ square matrix. It is clear that S depends on the frequency ω and the wave number β. If the periodic structure has no material loss, $\epsilon(y,z)$ is a real positive function, then energy is conserved and S is a unitary matrix. To obtain the scattering matrix S for given ω and β, it is necessary to solve Eq. (4) with proper boundary conditions.

The simplest and most important case is $\mathbb{M}=\{0\}$, namely the zeroth diffraction order is the only propagating order. In that case, S is a 2×2 matrix satisfying

$$\begin{bmatrix}b_0^+\\ b_0^-\end{bmatrix}=S\begin{bmatrix}a_0^+\\ a_0^-\end{bmatrix}. \tag{9}$$

Let s_{jk} be the (j,k) entry of above S. If, for a fixed β, $s_{11}(\omega)=0$ for a real frequency ω, then for an incident wave given above the periodic layer, there is no reflected wave. This is the simplest case of zero reflection and it is considered as a diffraction anomaly. If the structure is lossless, then the unitarity of S implies $|s_{21}(\omega)|=1$, and thus zero reflection implies total transmission. Similarly, if $s_{21}(\omega)=0$, then ω is the frequency for zero transmission for an incidence wave given above the periodic layer. If the periodic structure is lossless, then zero transmission implies total reflection. We also regard zero transmission as a diffraction anomaly. Popov *et al.* [4] first realized that structural symmetry is important to the appearance of zero reflection and zero transmission. In some cases, the frequency for these anomalies can be approximated [4,5,17,18]. However, even for periodic structures with the right symmetry, the existence of zero reflection or transmission has only been rigorously established for special circumstances [19,20].

For lossless structures, the power of incident waves is completely converted to outgoing waves. For $M=1$, that means $|a_0^+|^2+|a_0^-|^2=|b_0^+|^2+|b_0^-|^2$. If the structure has material loss, i.e., $\mathrm{Im}(\epsilon)$ is positive somewhere, then there could be a real frequency ω such that $b_0^+=b_0^-=0$ for some $(a_0^+,a_0^-)\neq(0,0)$. This is a case of perfect absorption [6,21,22] or coherent perfect absorption [23], and it is a useful diffraction anomaly for solar cell technology. Notice that perfect absorption corresponds to $S(\omega)$ being a singular matrix, and thus $\det S(\omega)=0$.

If there are two propagating diffraction orders, i.e., $M=2$, then S is a 4×4 matrix. For $\beta\in(0,\pi/L)$, we have $\mathbb{M}=\{0,-1\}$, namely the propagating orders correspond to wave numbers $\beta_0=\beta$ and $\beta_{-1}=\beta-2\pi/L$. We are interested in a diffraction anomaly where incident waves are given in the zeroth diffraction order and outgoing waves appear in the -1st diffraction order only. To write down a condition for this *blazing* diffraction phenomenon [7], we assume vectors

$\mathbf{a}^{\pm}$ and $\mathbf{b}^{\pm}$ are

$$\mathbf{a}^{\pm} = \begin{bmatrix} a^{\pm}_{-1} \\ a^{\pm}_{0} \end{bmatrix}, \quad \mathbf{b}^{\pm} = \begin{bmatrix} b^{\pm}_{-1} \\ b^{\pm}_{0} \end{bmatrix}, \tag{10}$$

and the entries of S are s_{jk} for $1 \leqslant j, k \leqslant 4$. The scattering matrix satisfies

$$\begin{bmatrix} b^{+}_{-1} \\ 0 \\ b^{-}_{-1} \\ 0 \end{bmatrix} = S \begin{bmatrix} 0 \\ a^{+}_{0} \\ 0 \\ a^{-}_{0} \end{bmatrix}. \tag{11}$$

The second and fourth rows of the above give

$$\begin{bmatrix} s_{22} & s_{24} \\ s_{42} & s_{44} \end{bmatrix} \begin{bmatrix} a^{+}_{0} \\ a^{-}_{0} \end{bmatrix} = \begin{bmatrix} 0 \\ 0 \end{bmatrix}. \tag{12}$$

Therefore,

$$\det \begin{bmatrix} s_{22} & s_{24} \\ s_{42} & s_{44} \end{bmatrix} = 0. \tag{13}$$

In summary, we have considered diffraction anomalies including zero reflection, zero transmission, perfect absorption, and blazing diffraction. In terms of the scattering matrix, each anomaly corresponds to a zero condition on an entry or a submatrix of the scattering matrix. The diffraction anomalies may occur at a specific frequency ω for a fixed structure and a fixed wave number β. In that case, all we have to do is to calculate ω by solving a scalar equation. If the incident angle is fixed, then β is related to ω, and the frequency is still the only unknown. Diffraction anomalies can also be studied for a fixed frequency, then the wave number β or incident angle is the unknown. However, for a fixed structure, some diffraction anomalies may not occur for any frequency or wave number. In that case, it is necessary to add tunable parameters to the structure and solve the parameters together with the frequency and/or wave number.

In principle, we can find diffraction anomalies by solving the equations obtained from the scattering matrix. Such a method works well if there are good initial guesses, but since good initial guesses are not easy to obtain, the method is not robust. Moreover, the method becomes computationally expensive if all diffraction anomalies in a given frequency or wave number interval are required. To obtain good initial guesses, it is necessary to densely scan the frequency or wave number interval. This implies that the diffraction problem must be solved repeatedly for many different values of the frequency or wave number, and this is computationally expensive.

III. NONLINEAR EIGENVALUE FORMULATIONS

To overcome the difficulty of finding good initial guesses for all diffraction anomalies in a given frequency or wavenumber interval, we develop a robust numerical method based on nonlinear eigenvalue formulations and a contour-integral method for solving nonlinear eigenvalue problems [15,16]. Although the diffraction of a time-harmonic wave is a BVP, the diffraction anomalies are special conditions of this BVP, and they can be reformulated as eigenvalue problems where the eigenvalue is the frequency or wave number. However, the eigenvalue problem is nonlinear with a nonlinearity in the eigenvalue. Fortunately, this type of NEPs can be accurately and robustly solved by the contour-integral method [15,16].

To describe the NEP formulations for various diffraction anomalies, we first consider the standard eigenvalue problem for resonant modes [24,25] and reformulate this linear eigenvalue problem as a NEP. In a 2D periodic structure given by a dielectric function $\epsilon(y, z)$ satisfying conditions (2) and (3), any E-polarized eigenmode is a Bloch mode,

$$u(y, z) = \phi(y, z)e^{i\beta y}, \tag{14}$$

where ϕ is periodic in y with period L and β is the Bloch wave number. The eigenvalue problem is for u satisfying Eq. (4) and proper boundary conditions as $z \to \pm\infty$. The eigenvalue is either ω (or $k_0 = \omega/c$, or k_0^2) for given real $\beta \in (-\pi/L, \pi/L]$ or β for given $\omega > 0$. We focus on the case where ω is the eigenvalue. If the boundary condition is $u \to 0$ as $z \to \pm\infty$, then the eigenmode is a guided mode. We are concerned with resonant modes (also called resonant states or quasinormal modes) for which u satisfies an outgoing radiation condition as $z \to \pm\infty$ [24,25]. This condition implies that power is radiated out to infinity as $z \to \pm\infty$, and ω must have a negative imaginary part, so that the mode amplitude decays with time.

For $|z| > d$, the nonzero electric-field component of a resonant mode can be expanded in plane waves, exactly like $u^{\pm}_{\text{sca}}$ in Eq. (7), namely

$$u(y, z) = \sum_{m\in\mathbb{Z}} c^{\pm}_m e^{i(\beta_m y \pm \gamma_m z)}, \quad \pm z \geqslant d, \tag{15}$$

where $c^{\pm}_m$ are the expansion coefficients, β_m and γ_m are given in Sec. II. However, k_0 is now complex with a negative imaginary part, $k_0^2 - \beta_m^2$ is in the lower half of the complex plane, the complex square root in

$$\gamma_m = \sqrt{k_0^2 - \beta_m^2} \tag{16}$$

should be defined using a branch cut along the negative imaginary axis (instead of the negative real axis), so that when $k_0^2 - \beta_m^2$ is in the third or fourth quadrant, γ_m is in the second or fourth quadrant, respectively. This choice of complex square root ensures that each term in the right-hand side of Eq. (15) is either an evanescent plane wave that decays exponentially as $z \to \pm\infty$ or an outgoing plane wave that radiates out power (and grows exponentially) as $z \to \pm\infty$. As in Sec. II, we have a set $\mathbb{M}$ for those integers m such that $k_0^2 - \beta_m^2$ is in the fourth quadrant. We assume $\mathbb{M}$ is not empty and contains 0. In that case, the resonant mode has the following far-field asymptotic expansion

$$u(y, z) \sim \sum_{m\in\mathbb{M}} c^{\pm}_m e^{i(\beta_m y \pm \gamma_m z)}, \quad z \to \pm\infty. \tag{17}$$

The linear eigenvalue problem of a resonant mode is for u satisfying Eq. (4) in Ω_{inf}, the far-field condition (17), and the following quasiperiodic conditions:

$$\begin{bmatrix} u \\ \partial_y u \end{bmatrix}_{y=L} = e^{i\beta L} \begin{bmatrix} u \\ \partial_y u \end{bmatrix}_{y=0}, \tag{18}$$

where Ω_{inf} is given by $0 < y < L$ and $-\infty < z < \infty$. Since the coefficients $c^{\pm}_m$ for $m \in \mathbb{M}$ are unknown, the far-field condition (17) is difficult to use. The standard approach is to use the perfectly matched layer technique [26–28], namely move

z to a path in the complex plane so that $u(y, z) \to 0$ as $z \to \infty$ along the path.

If we define a linear operator Λ_0 such that

$$\Lambda_0 e^{i\beta_m y} = i\gamma_m e^{i\beta_m y}, \quad m \in \mathbb{Z}, \tag{19}$$

then Eq. (15) gives rise to

$$\frac{\partial u}{\partial z} = \Lambda_0 u, \quad z = d, \tag{20}$$

$$\frac{\partial u}{\partial z} = -\Lambda_0 u, \quad z = -d. \tag{21}$$

The operator Λ_0 maps u (Dirichlet data) to the derivative of u (Neumann data) and is a so-called Dirichlet-to-Neumann operator. Since Λ_0 depends on ω and β, we obtain a NEP for u satisfying Eq. (4) in Ω_d and boundary conditions (18), (20), and (21), where Ω_d is the rectangular domain given by $0 < y < L$ and $-d < z < d$.

The above NEP formulation on Ω_d can be used for numerical implementation, but we prefer a NEP formulated on two line segments at $z = \pm d$ (for $0 < y < L$). To achieve this, we define a linear operator F that maps u at $z = \pm d$ (as functions of y for $0 < y < L$) to $\partial_z u$ at $z = \pm d$, where u satisfies Eq. (4) and boundary condition (18). The operator F depends on both β and ω and satisfies

$$F\mathbf{u} = \begin{bmatrix} \partial_z u(y, d) \\ \partial_z u(y, -d) \end{bmatrix}, \quad \mathbf{u} = \begin{bmatrix} u(y, d) \\ u(y, -d) \end{bmatrix}. \tag{22}$$

Let F be given in 2×2 blocks,

$$F = \begin{bmatrix} F_{11} & F_{12} \\ F_{21} & F_{22} \end{bmatrix}, \tag{23}$$

then Eqs. (20)–(22) lead to Eq. (1), where $A = A(\omega)$ is the 2×2 matrix operator

$$A = \begin{bmatrix} F_{11} - \Lambda_0 & F_{12} \\ F_{21} & F_{22} + \Lambda_0 \end{bmatrix}. \tag{24}$$

Equation (1) with the above A is our preferred NEP formulation for resonant modes. For given ω and β, the two operators Λ_0 and F can be approximated by matrices. If $y \in (0, L)$ is discretized by N points, then $\mathbf{u}$ is approximated by a column vector of length $2N$, Λ_0 and F are approximated by $N \times N$ and $(2N) \times (2N)$ matrices, respectively. In the Appendix, we give additional details on computing matrix approximations of Λ_0 and F. Since we assume β is given and ω is the unknown, we emphasize the dependence on ω by writing A as $A(\omega)$ in Eq. (1).

Next, we present NEP formulations for diffraction anomalies discussed in Sec. II. While the diffraction anomalies are most conveniently defined using the scattering matrix, their NEP formulations are derived from the governing Helmholtz equation and related boundary conditions. First, we consider a zero reflection where the incident wave is given above the periodic layer (i.e., for $z > d$) in the zeroth diffraction order and there is no reflected wave in the same diffraction order. Therefore, the total field for $|z| > d$ can be expanded as follows:

$$u = a_0^+ e^{i(\beta_0 y - \gamma_0 z)} + \sum_{m \neq 0} b_m^+ e^{i(\beta_m y + \gamma_m z)}, \ z > d, \tag{25}$$

$$u = \sum_{m \in \mathbb{Z}} b_m^- e^{i(\beta_m y - \gamma_m z)}, \ z < -d. \tag{26}$$

Clearly, u satisfies Eq. (21), the same boundary condition as the resonant modes, at $z = -d$. To obtain a boundary condition at $z = d$, we define a new linear operator Λ_1 by

$$\Lambda_1 e^{i\beta_m y} = \begin{cases} -i\gamma_0 e^{i\beta_0 y}, & m = 0, \\ i\gamma_m e^{i\beta_m y}, & m \neq 0, \end{cases} \tag{27}$$

and then u satisfies

$$\frac{\partial u}{\partial z} = \Lambda_1 u, \quad z = d. \tag{28}$$

Therefore, the NEP for zero reflection is Eq. (1) with a new matrix operator A given by

$$A = \begin{bmatrix} F_{11} - \Lambda_1 & F_{12} \\ F_{21} & F_{22} + \Lambda_0 \end{bmatrix}. \tag{29}$$

The case of zero transmission is somewhat more complicated. If an incident wave is given above the periodic layer in the zeroth diffraction order, and there is no transmitted wave in the zeroth diffraction order below the layer, then the total field is

$$u = a_0^+ e^{i(\beta_0 y - \gamma_0 z)} + \sum_{m \in \mathbb{Z}} b_m^+ e^{i(\beta_m y + \gamma_m z)}, \ z > d, \tag{30}$$

$$u = \sum_{m \neq 0} b_m^- e^{i(\beta_m y - \gamma_m z)}, \ z < -d. \tag{31}$$

Because of the incident wave, the boundary condition at $z = d$ is inhomogeneous. We have

$$\frac{\partial u}{\partial z} = \Lambda_0 u - 2ia_0^+ \gamma_0 e^{i(\beta_0 y - \gamma_0 d)}, \quad z = d. \tag{32}$$

Although $b_0^- = 0$, u still satisfies Eq. (21) at $z = -d$. The condition $b_0^- = 0$ implies that

$$\int_0^L u(y, -d) e^{-i\beta_0 y} \, dy = 0. \tag{33}$$

Combining the above with the operator F, we obtain a NEP given as Eq. (1) with a new matrix operator

$$A = \begin{bmatrix} F_{11} - \Lambda_0 & F_{12} & f(y) \\ F_{21} & F_{22} + \Lambda_0 & 0 \\ 0 & \mathrm{g} & 0 \end{bmatrix}, \tag{34}$$

and a new vector

$$\mathbf{u} = \begin{bmatrix} u(y, d) \\ u(y, -d) \\ 1 \end{bmatrix}, \tag{35}$$

where $f(y) = 2ia_0^+ \gamma_0 e^{i(\beta_0 y - \gamma_0 d)}$ and g is the linear functional that maps $u(y, -d)$ to the left-hand side of Eq. (33). When $y \in (0, L)$ is discretized by N points, $f(y)$ becomes by a column vector of length N, g is approximated by a row vector of length N, and A becomes a $(2N + 1) \times (2N + 1)$ matrix.

When the structure is absorptive, we can consider perfect absorption for which some incident waves do not produce any

outgoing propagating waves. If there is only one propagating diffraction order for each side of the periodic layer, then the total field can be written as

$$u = a_0^+ e^{i(\beta_0 y - \gamma_0 z)} + \sum_{m\neq 0} b_m^+ e^{i(\beta_m y + \gamma_m z)},\ z > d, \quad (36)$$

$$u = a_0^- e^{i(\beta_0 y + \gamma_0 z)} + \sum_{m\neq 0} b_m^- e^{i(\beta_m y - \gamma_m z)},\ z < -d. \quad (37)$$

Therefore, the boundary condition at $z = d$ is Eq. (28), the same as the zero reflection case considered above. The boundary condition at $z = -d$ is

$$\frac{\partial u}{\partial z} = -\Lambda_1 u, \quad z = -d. \quad (38)$$

Therefore, the NEP for perfect absorption is Eq. (1) with $\mathbf{u}$ given in (22), and A given by

$$A = \begin{bmatrix} F_{11} - \Lambda_1 & F_{12} \\ F_{21} & F_{22} + \Lambda_1 \end{bmatrix}. \quad (39)$$

For a lossless periodic structure, and if there are two propagating diffraction orders (the zeroth and negative-first orders if $0 < \beta \leqslant \pi/L$), we can consider a blazing diffraction phenomenon that converts all power of the incident waves (in zeroth diffraction order) to outgoing waves in the negative first order. The total field for $|z| > d$ has the same expansions (36) and (37). Therefore, the NEP formulation is also Eq. (1) with A given in Eq. (39) and $\mathbf{u}$ given in (22).

The NEP formulations above rely on operators F, Λ_0, and Λ_1. Alternative formulations can be derived using F^{-1}, Λ_0^{-1}, and Λ_1^{-1}. To find the diffraction anomalies based on these NEP formulations, it is necessary to find matrix approximations for these operators. For some numerical methods, F^{-1} is easier to obtain than F.

IV. CONTOUR-INTEGRAL METHOD

The contour-integral method for NEPs was originally developed by Asakura *et al.* [15]. The work of Beyn contains a simpler derivation and additional developments [16]. For the NEP given by Eq. (1), we assume A is a complex analytic matrix function of ω in a domain of the complex plane. In addition, we assume A is $n \times n$, and the NEP has k ($k < n$) distinct simple eigenvalues $\omega_1, \omega_2, \ldots, \omega_k$ inside a closed curve Γ (which itself is inside the domain where A is analytic). Let l be an integer such that $k < l \leqslant n$, and then the contour-integral method consists of the following steps [16]:

(1) For a random complex $n \times l$ matrix R, evaluate

$$A_0 = \frac{1}{2\pi i}\int_\Gamma A^{-1}(\omega) R\, d\omega,$$

$$A_1 = \frac{1}{2\pi i}\int_\Gamma \omega A^{-1}(\omega) R\, d\omega.$$

(2) Find the singular value decomposition of A_0, i.e.,

$$A_0 = P\Sigma Q^*,$$

where P is an $n \times n$ unitary matrix, Q is an $l \times l$ unitary matrix, Q^* is the conjugate transpose of Q, and Σ is a diagonal matrix with diagonal entries satisfying $\sigma_1 \geqslant \sigma_2 \geqslant \cdots \geqslant \sigma_l \geqslant 0$.

(3) Let P_0 be the first k columns of P, Q_0 be the first k columns of Q, Σ_0 be the leading $k \times k$ diagonal block of Σ, evaluate

$$B = P_0^* A_1 Q_0 \Sigma_0^{-1}.$$

(4) Find the eigenvalues and eigenvectors of matrix B. If ω_j and $\mathbf{s}_j$ (for $1 \leqslant j \leqslant k$) are the eigenvalues and eigenvectors of B, then the eigenvalues and eigenvectors of the NEP are ω_j and $\mathbf{u}_j = P_0 \mathbf{s}_j$ for $1 \leqslant j \leqslant k$, respectively.

In the following, we give a brief explanation for the above method. By the definition of NEP, if ω_j is an eigenvalue, then $A(\omega_j)$ is singular, and there are nonzero vectors $\mathbf{u}_j$ (the eigenvector) and $\mathbf{v}_j$ (the left eigenvector), such that $A(\omega_j)\mathbf{u}_j = \mathbf{0}$ and $\mathbf{v}_j^* A(\omega_j) = \mathbf{0}$. If ω_j is a simple eigenvalue, then the nullspace and left nullspace of $A(\omega_j)$ are one dimensional, and $\mathbf{u}_j$ and $\mathbf{v}_j$ can be scaled such that

$$\mathbf{v}_j^* A'(\omega_j)\mathbf{u}_j = 1,$$

where A' is the derivative of A with respect to ω. Moreover, it is necessary to assume that the k eigenvectors $\mathbf{u}_1, \mathbf{u}_2, \ldots, \mathbf{u}_k$ are linearly independent, and the k left eigenvectors are also linearly independent.

Using Keldysh's theorem [16], it can be proved that

$$A_0 = \sum_{j=1}^{k} \mathbf{u}_j \mathbf{v}_j^* R = UV^* R,$$

$$A_1 = \sum_{j=1}^{k} \omega_j \mathbf{u}_j \mathbf{v}_j^* R = U\Lambda V^* R,$$

where $U = [\mathbf{u}_1, \mathbf{u}_2, \ldots, \mathbf{u}_k]$, $V = [\mathbf{v}_1, \mathbf{v}_2, \ldots, \mathbf{v}_k]$, and

$$\Lambda = \begin{bmatrix} \omega_1 & & & \\ & \omega_2 & & \\ & & \ddots & \\ & & & \omega_k \end{bmatrix}.$$

Notice that $\mathrm{rank}(U) = \mathrm{rank}(V) = \mathrm{rank}(V^*) = k$. Since R is random, we assume $\mathrm{rank}(V^*R)$ is also k. This implies that $\mathrm{rank}(A_0) = k$. Therefore, $\sigma_k \neq 0$, $\sigma_j = 0$ for $j > k$, and

$$A_0 = UV^*R = P\Sigma Q^* = P_0 \Sigma_0 Q_0^*.$$

The above gives rise to $\mathrm{range}(A_0) = \mathrm{range}(U) = \mathrm{range}(P_0)$. Therefore, there is a nonsingular matrix S, such that $U = P_0 S$, and thus

$$S = P_0^* U, \quad S(V^* R Q_0 \Sigma_0^{-1}) = I.$$

Therefore,

$$B = P_0^*(U\Lambda V^* R) Q_0 \Sigma_0^{-1} = S\Lambda S^{-1}.$$

The above is an eigenvalue decomposition for matrix B and S is the matrix of eigenvectors of B.

In practice, k is not known *a priori*. If l is sufficiently large, then we can determine k numerically from the singular values of A_0, i.e., by the conditions $\sigma_k > 0$ and $\sigma_{k+1} \approx 0$. If σ_l is not close to zero, then it is necessary to repeat the calculation with a larger l. The method can also be extended to the case where k is larger than n (the size of matrix A) [16].

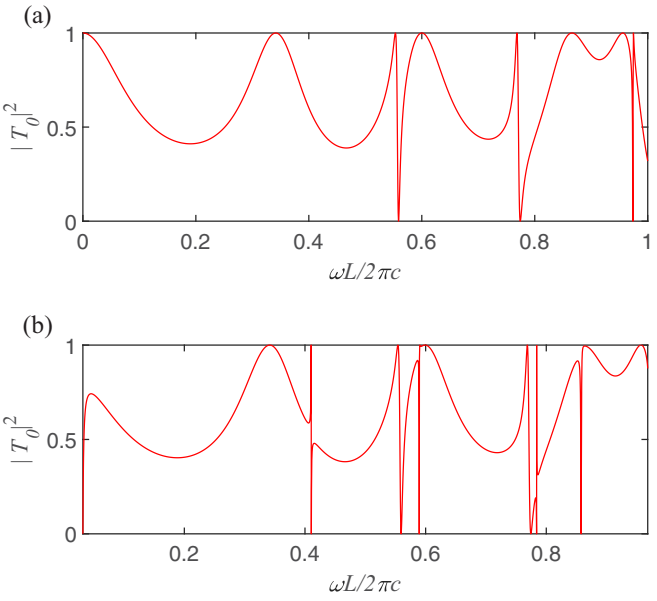

FIG. 1. Transmission spectra of a periodic array of circular cylinder with radius $a = 0.3L$ and dielectric constant $\epsilon_1 = 11.6$ for, (a) a normal incident wave and $\omega L/(2\pi c) \in (0, 1)$, (b) an incident plane wave with $\beta = 0.2/L$ and $\omega L/(2\pi c) \in (0.1/\pi, 1 - 0.1/\pi)$.

V. NUMERICAL EXAMPLES

To illustrate our method, we consider a periodic array of dielectric cylinders surrounded by air. The radius and the dielectric constant of the cylinders are a and ϵ_1, respectively. The cylinders are parallel to the x axis. Their centers are located on the y axis. The period L of the array is the distance between the centers of two nearby cylinders. The array is considered as a periodic layer with a thickness $2d = L$. For all numerical examples, we discretize the interval $(0, L)$ by $N = 11$ points. Therefore, the operators Λ_0 and Λ_1 are approximated by 11×11 matrices, and the operator F is approximated by a 22×22 matrix, and the matrix A is either 22×22 or 23×23. When the contour-integral method is used to solve the NEP, we use 100 points to discretize the contour and approximate integrals along the contour by the trapezoid method. The contour-integral method requires a random matrix R which has the same number of rows as matrix A and l columns. For all numerical examples in this section, we choose $l = 10$.

First, we consider the periodic array with $a = 0.3L$ and $\epsilon_1 = 11.6$. In Fig. 1, we show the transmission spectra for plane incident waves with wave number $\beta = 0$ (normal incidence) and $\beta = 0.2/L$. The frequency interval is chosen so that there is exactly one propagating diffraction order. The incident wave is given above the array, and thus $a_0^+ \neq 0$, $a_0^- = 0$, and the transmission coefficient is $T_0 = s_{21} = b_0^-/a_0^+$. From Fig. 1, it appears that total transmission (zero reflection) and zero transmission occur at some special frequencies. To find the frequencies for zero reflection or transmission and the resonant modes, we use the contour-integral method with a circular contour in the complex plane of ω centered on the real axis. In Table I, we show seven resonant modes for $\beta = 0$ and $\beta = 0.2/L$, respectively. The results are obtained using a contour with center at $0.7(2\pi c/L)$ and radius $0.2(2\pi c/L)$. Notice that for $\beta = 0$ there are three special resonant modes with a real frequency (shown in italics in Table I). They are examples of bound states in the continuum (BICs) [29–36]. A BIC has the same expansion, Eq. (15), as the resonant modes, but $c_m^{\pm} = 0$ for any m such that γ_m is real. For the three BICs in Table I, since $\mathbb{M} = \{0\}$, only $c_0^{\pm} = 0$. Although a BIC does not radiate out power as $z \to \pm\infty$, it satisfies the same boundary conditions and the same NEP formulation as the resonant modes. The three BICs in Table I are standing waves with $\beta = 0$, and they turn to resonant modes with a high Q factor as β moves away from zero.

TABLE I. Frequencies of resonant modes in a periodic array of circular cylinders with $a = 0.3L$ and $\epsilon_1 = 11.6$ for wave number $\beta = 0$ and $0.2/L$.

$\omega L/(2\pi c)$ for $\beta = 0$	$\omega L/(2\pi c)$ for $\beta = 0.2/L$
0.557333–0.002647i	0.557898–0.002502i
0.589733	0.589439–0.000147i
0.593629–0.058809i	0.593758–0.058677i
0.770917–0.002940i	0.771034–0.002876i
0.784154	0.784059–0.000061i
0.858999	0.857857–0.000543i
0.857873–0.054473i	0.857930–0.054206i

In Table II, we list zero-reflection frequencies for both $\beta = 0$ and $\beta = 0.2/L$. In Fig. 1, we can find seven and nine total-transmission frequencies in $(0, 2\pi c/L)$ for $\beta = 0$ and $\beta = 0.2/L$, respectively. In Table II, only four and five zero-reflection frequencies are listed, since they are the ones inside the contour chosen for the computation. For $\beta = 0$, we use the same circular contour as before [with center at $0.7(2\pi c/L)$ and radius $0.2(2\pi c/L)$] and obtain all four zero-reflection frequencies in the interval $(0.5, 0.9)(2\pi c/L)$, as well as three BICs listed in Table I. Interestingly, the BICs also satisfy the boundary conditions for the zero reflection solutions. For $\beta = 0.2/L$, the chosen contour is centered at $0.65(2\pi c/L)$ and has a radius $0.15(2\pi c/L)$, and thus the obtained zero-reflection frequencies belong to the interval $(0.5, 0.8)(2\pi c/L)$.

From Fig. 1, it appears that there are three and six zero-transmission frequencies in the interval $(0, 2\pi c/L)$ for $\beta = 0$ and $\beta = 0.2/L$, respectively. To find all zero-transmission frequencies in $(0.3, 0.9)(2\pi c/L)$, we use a circular contour with center at $0.6(2\pi c/L)$ and radius $0.3(2\pi c/L)$. The results are listed in Table III for both $\beta = 0$ and $\beta = 0.2/L$. The NEP for zero transmission, i.e., Eq. (1) for A given in (34), is also

TABLE II. Frequencies of zero reflection in a periodic array circular cylinders with $a = 0.3L$ and $\epsilon_1 = 11.6$ for wave number $\beta = 0$ and $0.2/L$.

$\omega L/(2\pi c)$ for $\beta = 0$	$\omega L/(2\pi c)$ for $\beta = 0.2/L$
0.553305	0.554087
0.600099	0.590294
0.768452	0.599160
0.865895	0.768661
—	0.784094

TABLE III. Frequencies of zero transmission in a periodic array circular cylinders with $a = 0.3L$ and $\epsilon_1 = 11.6$ for wave number $\beta = 0$ and $0.2/L$.

$\omega L/(2\pi c)$ for $\beta = 0$	$\omega L/(2\pi c)$ for $\beta = 0.2/L$
0.558859	0.410497
0.774310	0.559341
—	0.589390
—	0.774413
—	0.783940
—	0.857738

satisfied by the BICs, but unlike that given in Eq. (35), for a BIC, the last entry of $\mathbf{u}$ is zero. For $\beta = 0$, the numerical results include two zero-transmission frequencies listed in Table III and four BICs [three listed in Table I and a new one with frequency $\omega = 0.411228(2\pi c/L)$]. Of course, the computed vector $\mathbf{u}$ is scaled differently, its last entry is not simply 1 or 0. However, the BICs can be easily identified by considering the ratio between the last entry and the entry with the maximum magnitude. In our case, the ratio for the four BICs ranges from $\mathcal{O}(10^{-9})$ to $\mathcal{O}(10^{-7})$. The contour-integral method generally gives complex solutions for ω. For the two zero-transmission frequencies of $\beta = 0$ in Table III, the imaginary part of the normalized frequency $\omega L/(2\pi c)$ is $\mathcal{O}(10^{-11})$. For $\beta = 0.2/L$, the numerical solutions are less accurate, but $\mathrm{Im}(\omega)L/(2\pi c)$ is still bounded by 4.4×10^{-5} for all cases listed in the right column of Table III.

Next, we consider perfect absorption of normal incident waves ($\beta = 0$) in a periodic array of circular cylinders with material loss, where ϵ_1 (the dielectric constant of the cylinders) is complex. However, for a fixed ϵ_1 and a fixed radius a, perfect absorption does not usually occur, and the NEP problem for A given in Eq. (39) has only complex-ω solutions. To find perfect absorption for the periodic array, we have to tune a structural or material parameter. For example, if $a = 0.3L$ is fixed and the refractive index of the cylinders is $n_1 = \sqrt{\epsilon_1} = \sqrt{11.6} + i\sigma$, where σ is a parameter, then perfect absorption occurs at $\sigma = 0.0142765$ with a real frequency $\omega = 0.770981(2\pi c/L)$. This result is obtained iteratively with an iteration in σ. In each iteration (i.e., for a given σ), we solve the NEP using a circular contour (in the complex ω plane) with center $0.8(2\pi c/L)$ and radius $0.1(2\pi c/L)$ and find a solution ω which is complex in general. The iterative process can be regarded as a root-finding method for solving $\mathrm{Im}(\omega) = 0$. We can also find perfect absorption by tuning the radius a for a fixed complex ϵ_1. In Table IV, we list a few cases where the imaginary part of n_1 is specified. The results are obtained using a circular contour with center $0.7(2\pi c/L)$ and radius $0.2(2\pi c/L)$.

TABLE IV. Radius a and frequency ω for perfect absorption in a periodic array of lossy circular cylinders with refractive index $n_1 = \sqrt{11.6} + i\sigma$.

$\sigma = \mathrm{Im}(n_1)$	a/L	$\omega L/(2\pi c)$
0.012	0.322575	0.715869
0.013	0.312982	0.738371
0.014	0.302888	0.763499
0.015	0.292248	0.791757

Finally, we consider blazing diffraction for a periodic array of cylinders with radius $a = 0.3L$ and dielectric constant $\epsilon_1 = 15.42$ and concentrate on the case of two propagating diffraction orders with wave numbers $\beta = \beta_0 = \pi/L$ and $\beta_{-1} = -\pi/L$. Using a circular contour with center $0.65(2\pi c/L)$ and radius $0.11(2\pi c/L)$, we find the following five frequencies:

$$0.549336,\ 0.670542,\ 0.678285,\ 0.686822,\ 0.745395.$$

Since the periodic array has a mirror symmetry in z, the blazing diffraction solutions are either even or odd in z. Among the five solutions above, the first three are even in z and the last two are odd in z.

We have repeated some calculation using different values of N [for discretizing the interval $(0, L)$] and different number of points for discretizing the contour. Typically, $N = 9$ is sufficient to give four significant digits. When N is increased to 11, the accuracy is improved by at least a factor of two. For discretizing the contour, 100 points is more than enough. Typical numerical results obtained with 100 and 200 points for the contour have more than eight identical digits.

VI. CONCLUSION

Diffraction anomalies such as zero reflection, zero transmission, perfect absorption, and blazing diffraction are interesting wave phenomena with important applications. Existing methods for computing the diffraction anomalies either scan the frequency (or wave number or other parameters) densely or determine the frequency iteratively, and, thus, they are computationally expensive and not very reliable. Our method based on NEP formulations and a contour-integral method is capable of finding all diffraction anomalies in a given frequency interval. Since the NEPs involve small matrices and no initial guesses for the frequency are needed, our method is efficient and robust. Although the method is only formulated for E-polarized waves in 2D structures with a single periodic direction, it can be easily generalized to full-vector waves in 3D structures with two periodic directions. It is also straightforward to extend the method to other diffraction anomalies. The method provides a useful tool for analyzing diffraction anomalies and explore their applications.

ACKNOWLEDGMENT

The authors acknowledge support from the Research Grants Council of Hong Kong Special Administrative Region, China (Grant No. CityU 11304619).

APPENDIX: MATRIX APPROXIMATION OF Λ_0 AND F

Here we briefly describe a semianalytic method for approximating operators Λ_0 and F. The method was originally presented in Refs. [11] and [37], and it is applicable to periodic arrays of circular cylinders. Let L be the period of the array and a and n_1 be the radius and refractive index of the cylinders, respectively. For $d = L/2$, Ω_d is a square

given by $0 < y < L$ and $-d < z < d$. We assume a cylinder is contained in Ω_d and centered at $(y, z) = (L/2, 0)$.

Let $N = 2p + 1$ be a positive odd integer and $y_j = L(j - 0.5)/N$ for $1 \leqslant j \leqslant N$. For $z \geqslant d$, the field expansion (15) may be approximated by

$$u(y, z) \approx \sum_{m=-p}^{p} c_m^+ e^{i(\beta_m y + \gamma_m z)}, \quad z \geqslant d. \tag{A1}$$

Evaluating the above at $(y, z) = (y_j, d)$, we obtain an $N \times N$ matrix C_1, such that

$$\mathbf{u}^+ \approx C_1 \mathbf{c}^+,$$

where $\mathbf{u}^+$ is a column vector of $u(y_j, d)$ for $1 \leqslant j \leqslant N$ and $\mathbf{c}^+$ is a column vector of c_m^+ for $-p \leqslant m \leqslant p$. We can also take a derivative with respect to z for the approximate expansion above and evaluate the result at (y_j, d) for $1 \leqslant j \leqslant N$. This gives rise to a matrix C_2 such that

$$\partial_z \mathbf{u}^+ \approx C_2 \mathbf{c}^+,$$

where $\partial_z \mathbf{u}^+$ is a vector for $\partial_z u(y_j, d)$. The operator Λ_0 is then approximated by the $N \times N$ matrix $C_2 C_1^{-1}$.

Inside Ω_d, the general solution Eq. (4) is

$$u(y, z) = \sum_{m=-\infty}^{+\infty} d_m \phi_m(r) e^{im\theta}, \tag{A2}$$

where (r, θ) are the polar coordinates satisfying

$$y = L/2 + r\cos\theta, \quad z = r\sin\theta,$$

and ϕ_m is a particular solution with a scaled cylindrical wave incident on the cylinder. More specifically, $\phi_m(r) = A_m J_m(k_0 n_1 r)$ for $r < a$ and $\phi_m(r) = B_m H_m^{(1)}(k_0 r) + H_m^{(2)}(k_0 r)/H_m^{(2)}(k_0 a)$ for $r > a$, where J_m, $H_m^{(1)}$, $H_m^{(2)}$ are mth-order Bessel and Hankel functions. The coefficients A_m and B_m can be solved from the condition that ϕ_m and $d\phi_m/dr$ are continuous at $r = a$. Now, we approximate the expansion by $4N$ terms:

$$u(y, z) \approx \sum_{m=-2N}^{2N-1} d_m \phi_m(r) e^{im\theta}. \tag{A3}$$

From the above, we can take partial derivatives and find the approximate expansions for $\partial_y u$ and $\partial_z u$. Let $z_k = -L/2 + L(k - 0.5)/N$ for $k = 1, 2, \ldots, N$. Evaluating u by Eq. (A3) at (y_j, d), $(y_j, -d)$ for $1 \leqslant j \leqslant N$ and $(0, z_k)$ and (L, z_k) for $1 \leqslant k \leqslant N$, we obtain a $(4N) \times (4N)$ matrix D_1 mapping a column vector $\mathbf{d}$ (for d_m, $-2N \leqslant m < 2N - 1$) to a column vector of length $4N$ for u at the $4N$ sampling points on the boundary of Ω_d. Similarly, we can evaluate $\partial_z u$ at $(y_j, \pm d)$ for $1 \leqslant j \leqslant N$ and evaluate $\partial_y u$ at $(0, z_k)$ and (L, z_k) for $1 \leqslant k \leqslant N$, and obtain a $(4N) \times (4N)$ matrix D_2 that maps vector $\mathbf{d}$ to a vector of length $4N$ for the normal derivative of u at the $4N$ points on the boundary of Ω_d. Therefore, $D_2 D_1^{-1}$ is a $(4N) \times (4N)$ matrix mapping u to the normal derivative of u at the $4N$ points on the boundary of Ω_d. To reduce the numerical error caused by the possible ill conditioning of D_1, we normalize the columns of D_1 to obtain $\hat{D}_1 = D_1 S$, where the columns of $\hat{D}_1$ are unit vectors and S is a diagonal matrix, evaluate $\hat{D}_2 = D_2 S$, and replace $D_2 D_1^{-1}$ with $\hat{D}_2 \hat{D}_1^{-1}$. Finally, we can use the quasiperiodic condition (18) to eliminate u and $\partial_y u$ at $y = 0$ and $y = L$. The final result is a $(2N) \times (2N)$ matrix F satisfying

$$\begin{bmatrix} \partial_z \mathbf{u}^+ \\ \partial_z \mathbf{u}^- \end{bmatrix} = F \begin{bmatrix} \mathbf{u}^+ \\ \mathbf{u}^- \end{bmatrix}, \tag{A4}$$

where $\mathbf{u}^-$ and $\partial_z \mathbf{u}^-$ are column vectors of $u(y_j, -d)$ and $\partial_z u(y_j, -d)$ for $1 \leqslant j \leqslant N$, respectively.

[1] R. W. Wood, On the remarkable case of uneven distribution of a light in a diffractive grating spectrum, Lond. Edinb. Dubl. Philos. Mag. J. Sci. **4**, 396 (1902).

[2] U. Fano, The theory of anomalous diffraction gratings and of quasi-stationary waves on metallic surfaces (Sommerfield's waves), J. Opt. Soc. Am. **31**, 213 (1941).

[3] A. Hessel and A. A. Oliner, A new theory of Wood's anomalies on optical gratings, Appl. Opt. **4**, 1275 (1965).

[4] E. Popov, L. Mashev, and D. Maystre, Theoretical study of the anomalies of coated dielectric gratings, Optica Acta **33**, 607 (1986).

[5] S. Fan, W. Suh, and J. D. Joannopoulos, Temporal coupled-mode theory for Fano resonant mode in optical resonators, J. Opt. Soc. Am. A **20**, 569 (2003).

[6] M. C. Hutley and D. Maystre, The toal absorption of light by a diffraction grating, Opt. Commun. **19**, 431 (1976).

[7] E. Popov, B. Bozhkov, and M. Neviére, Almost perfect blazing by photonic crystal rod gratings, Appl. Opt. **40**, 2417 (2001).

[8] A. Krasnok, D. Baranov, H. Li, M.-A. Miri, F. Monticone, and A. Alú, Anomalies in light scattering, Adv. Opt. Photon. **11**, 892 (2019).

[9] L. Li, New formulation of the Fourier modal method for crossed surface-relief gratings, J. Opt. Soc. Am. A **14**, 2758 (1997).

[10] G. Bao, Z. Chen, and H. Wu, Adaptive finite-element method for diffraction gratings, J. Opt. Soc. Am. A **22**, 1106 (2005).

[11] Y. Huang and Y. Y. Lu, Scattering from periodic arrays of cylinders by Dirichlet-to-Neumann maps, J. Lightw. Technol. **24**, 3448 (2006).

[12] G. Bao, P. Li, and H. Wu, An adaptive edge element method with perfectly matched absorbing layers for wave scattering by biperiodic structures, Math. Comp. **79**, 1 (2010).

[13] Y. He, P. Li, and J. Shen, A new spectral method for numerical solution of the unbounded rough surface scattering problem, J. Comput. Phys. **275**, 608 (2014).

[14] W. Lu and Y. Y. Lu, Efficient high order waveguide mode solvers based on boundary integral equations, J. Comput. Phys. **272**, 507 (2014).

[15] J. Asakura, T. Sakurai, H. Tadano, T. Ikegami, and K. Kimura, A numerical method for nonlinear eigenvalue problems using contour integrals, JSIAM Lett. **1**, 52 (2009).

[16] W.-J. Beyn, An integral method for solving nonlinear eigenvalue problems, Lin. Algebr. Appl. **436**, 3839 (2012).

[17] C. Blanchard, J.-P. Hugonin, and C. Sauvan, Fano resonant modes in photonic crystal slabs near optical bound states in the continuum, Phys. Rev. B **94**, 155303 (2016).
[18] H. Wu, L. Yuan, and Y. Y. Lu, Approximating transmission and reflection spectra near isolated nondegenerate resonances, Phys. Rev. A **105**, 063510 (2022).
[19] S. P. Shipman and H. Tu, Total resonant transmission and reflection by periodic structures, SIAM J. Appl. Math. **72**, 216 (2012).
[20] L. Yuan, M. Zhang, and Y. Y. Lu, Real transmission and reflection zeros of periodic structures with a bound state in the continuum, Phys. Rev. A **106**, 013505 (2022).
[21] E. Popov, D. Maystre, R. C. McPhedran, M. Nevière, M. C. Hutley, and G. H. Derrick, Total absorption of unpolarized light by crossed gratings, Opt. Express **16**, 6146 (2008).
[22] N. I. Landy, S. Sajuyigbe, J. J. Mock, D. R. Smith, and W. J. Padilla, Perfect Metamaterial Absorber, Phys. Rev. Lett. **100**, 207402 (2008).
[23] Y. D. Chong, L. Ge, H. Cao, and A. D. Stone, Coherent Perfect Absorbers: Time-Reversed Lasers, Phys. Rev. Lett. **105**, 053901 (2010).
[24] S. Fan and J. D. Joannopoulos, Analysis of guided resonances in photonic crystal slabs, Phys. Rev. B **65**, 235112 (2002).
[25] A. Abdrabou and Y. Y. Lu, Indirect link between resonant and guided modes on uniform and periodic slabs, Phys. Rev. A **99**, 063818 (2019).
[26] J. P. Berenger, A perfectly matched layer for the absorption of electromagnetic waves, J. Comput. Phys. **114**, 185 (1994).
[27] W. C. Chew and W. H. Weedon, A 3-D perfectly matched medium from modified Maxwell's equations with stretching coordinates, Microw. Opt. Technol. Lett. **7**, 599 (1994).
[28] S. Hyun, J. Hwang, Y. Lee, and S. Kim, Computation of resonant modes of open resonators using the FEM and the anisotropic perfectly matched layer boundary condition, Microw. Opt. Technol. Lett. **16**, 352 (1997).
[29] C. W. Hsu, B. Zhen, A. D. Stone, J. D. Joannopoulos, and M. Soljačić, Bound states in the continuum, Nat. Rev. Mater. **1**, 16048 (2016).
[30] A. F. Sadreev, Interference traps waves in an open system: bound states in the continuum, Rep. Prog. Phys. **84**, 055901 (2021).
[31] S. Venakides and S. Venakides, Resonance and bound states in photonic crystal slabs, SIAM J. Appl. Math. **64**, 322 (2003).
[32] R. Porter and D. Evans, Embedded Rayleigh-Bloch surface waves along periodic rectangular arrays, Wave Motion **43**, 29 (2005).
[33] D. C. Marinica, A. G. Borisov, and S. V. Shabanov, Bound States in the Continuum in Photonics, Phys. Rev. Lett. **100**, 183902 (2008).
[34] C. W. Hsu, B. Zhen, J. Lee, S.-L. Chua, S. G. John- son, J. D. Joannopoulos, and M. Soljačić, Observation of trapped light within the radiation continuum, Nature (Lond.) **499**, 188 (2013).
[35] E. N. Bulgakov and A. F. Sadreev, Bloch bound states in the radiation continuum in a periodic array of dielectric rods, Phys. Rev. A **90**, 053801 (2014).
[36] Z. Hu and Y. Y. Lu, Standing waves on two-dimensional periodic dielectric waveguides, J. Opt. **17**, 065601 (2015).
[37] J. Yuan and Y. Y. Lu, Photonic bandgap calculations with Dirichlet-to-Neumann maps, J. Opt. Soc. Am. A **23**, 3217 (2006).